7th International Conference on Debris-Flow Hazards Mitigation

Commonalities between debris flows and flow failures

Robb Eric S. Moss, Ph.D., P.E., F.ASCE [a,]*

[a]Prof. Dept Civil and Environmental Engineering, Cal Poly, San Luis Obispo, CA 93401

Abstract

Debris flow and flow failure are terms used to describe large displacement slope failures. The initiation or triggering often differs due to the nature and state of the material, but once triggered these two failure mechanisms both tend to behave like a Bingham plastic exhibiting a yield strength and a strain-rate dependent strength. In this paper the rheology of these failures is examined and compared to field data and lab data to find commonalities. A future goal is to move towards a common definition of the physics and a joint empirical database for improved statistics and predictive models. The authors own field investigations in Chile and lab investigations using shake table experiments will be reviewed along with studies by other researchers.

Keywords: flow failure; debris flow; liquefaction; residual strength; steady state; critical state; mine tailings; colluvium

1. Introduction

Debris flows and flow failures are both forms of particulate behavior that result in flows with large runout distances, ranging from 10's to 1000's of meters (Hungr, 1995; Iverson, 1997; Yazdi & Moss, 2015). Debris flow typically describes failure of a naturally deposited heterogeneous coarse grained material (e.g., colluvium) that has been triggered by a high intensity rainfall event or other mechanism resulting in rapid flow-type behavior. Flow failure typically describes failure of a man-made material (e.g., mine tailings) or uniform natural material (e.g., sand) that has been triggered statically or seismically resulting in rapid flow-type behavior. In both failure mechanisms the bulk soil/rock mass fluidizes, resulting in low shear strength and little resistance to deformation. Triggering of these failure mechanism can come about in many different ways, and the runout is a function of several specific mass and intergranular conditions, but the flow phase of these failures are physically the same. In this paper the commonalities and differences of debris flows and flow failures are explored to arrive at some understanding of the physics. Then some recent studies are discussed that evaluate the flow characteristics of fluidized particulate material.

2. Flow Commonalities

Debris flows and flow failures can be triggered in a number of different ways, and can exhibit different amounts of runout, but both failures have similar flow characteristics (Iverson et al., 1997; Sassa, 2000; Kramer, 1988; Hungr, 1995). Figure 1 shows a schematic separating the triggering, from the flow, and the runout. The following discussion will define these terms and their physics.

The flow phase of both debris flows and flow failures can be characterized as steady state shearing with excess pore pressures (Figure 2a). Steady state meaning that the critical void ratio ($e_{critical}$) has been reached where no further contraction or dilation is needed to continue shearing the soil (Schofield & Wroth, 1968) at a residual shear strength ($\tau_{residual}$). With the addition of excess pore pressures the soil can exhibit flow-like behavior.

This behavior is consistent for both uniform (e.g., beach sand) and non-uniform (e.g., colluvium) materials. The shear strength (τ), or the shear stress at which the soil "fails", is generally defined by the contributions of any cohesion (c) and stress dependent (σ_n') inter-particle friction (ϕ') as shown in Equation 1 (Terzaghi, 1951). In the case of granular material, the cohesion term is often negligible.

* Corresponding author: rmoss@calpoly.edu

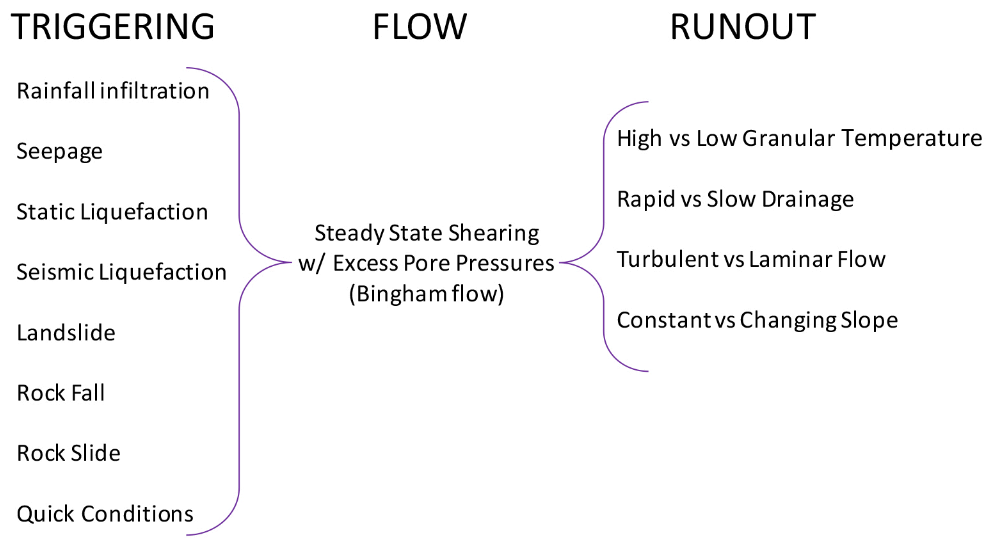

$$\tau = c + \sigma_n' tan\phi' \tag{1}$$

The stress dependence is influenced by the pore pressure (u) as shown in Equation 2 (Terzaghi, 1951) where (σ_n') is the normal effective stress and (σ_n) is the normal total stress. Pore pressures will increase to the point that the frictional forces are reduced below some threshold, allowing the soil to flow.

$$\sigma_n' = \sigma_n - u \tag{2}$$

Sufficiently sheared particulate materials approach a stead state response regardless of if they have the capacity to initially dilate or contract (Figure 2a). Once steady state is achieved and if excess pore pressure are sufficient the material can approach a flow threshold. The threshold to flow is often represented in terms of non-Newtonian flow as shown in Figure2b. If we restrict flow to laminar conditions (Reynolds number, R_e<5) then we can treat the fluid as visco-plastic (i.e., Bingham plastic). The characteristic of a non-Newtonian fluid like a Bingham plastic is that it has

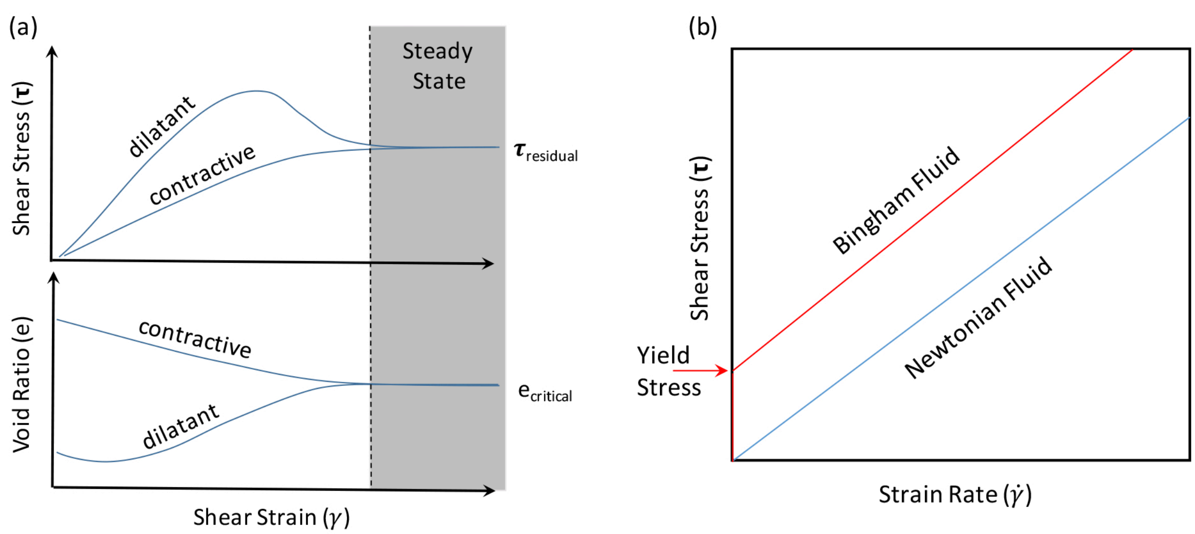

Figure 2. (a) Qualitative plot of dilatant and contractive behaviour of granular soils when subjected to shearing. Sufficient shearing will result in a steady state response at a critical void ratio and a residual shear strength. (b) Diagram showing Newtonian and Non-Newtonian fluid response to strain rate. A non-Newtonian fluid such as a Bingham fluid will deform after the shear stress exceeds a material specific yield stress.

some limiting yield strength followed by a strain rate ($\dot{\gamma}$) dependent shear strength. This behavior is typically explained in a physical manner by stating that the fluid has particles that provide some limiting stress threshold.

3. Triggering and Runout Dissimilarities.

If flow can be posited as the same for debris flows and flow failures, what of the triggering and runout? Here the two failure mechanisms differ greatly. The triggering can come about in many different ways, all resulting in steady state behavior with excess pore pressures. Whether the material starts out as dilatant colluvium (Anderson and Sitar, 1995) or contractive mine waste (Bryant, Duncan, and Seed, 1983) the steady state flow behavior can be described the same. Figure 3 is a conceptual summary of lab tests showing both contractive and dilatant materials achieving the critical state line.

Runout distance from a hazard perspective is an important parameter to be able to forecast. Unfortunately the complexity of the physics has so far rendered this a daunting task (Lucia, Duncan, and Seed, 1981; Jeyapalan, Duncan, and Seed, 1983a and b; Bryant, Duncan, and Seed, 1983; Hungr, 1995; Iverson et al., 2010). The duration in which the material remains in a fluidized state is a primary variable that controls runout distance. This is influenced by any change in slope, two dimensional effects of topography, the presence of an impeding or impermeable layer above/below the fluidized soil, if the flow is behavior is laminar or turbulent, the granular "temperature" or granular kinetics, and possibly other variables. Granular temperature (Iverson, 1997) is a term that describes behavior of heterogeneous particle sized materials that during flow tend to translate potential energy (slope) into kinetic energy (relative particle dilation) that results in continued capacity of the material to contract and generate more excess pore pressures. Hungr (1995) proposed a model that has been shown to capture runout for flow failures in tailings material adequately for most simple 2D situations based on back-analysis of field case histories. More complex geometries and source materials have not been as well captured.

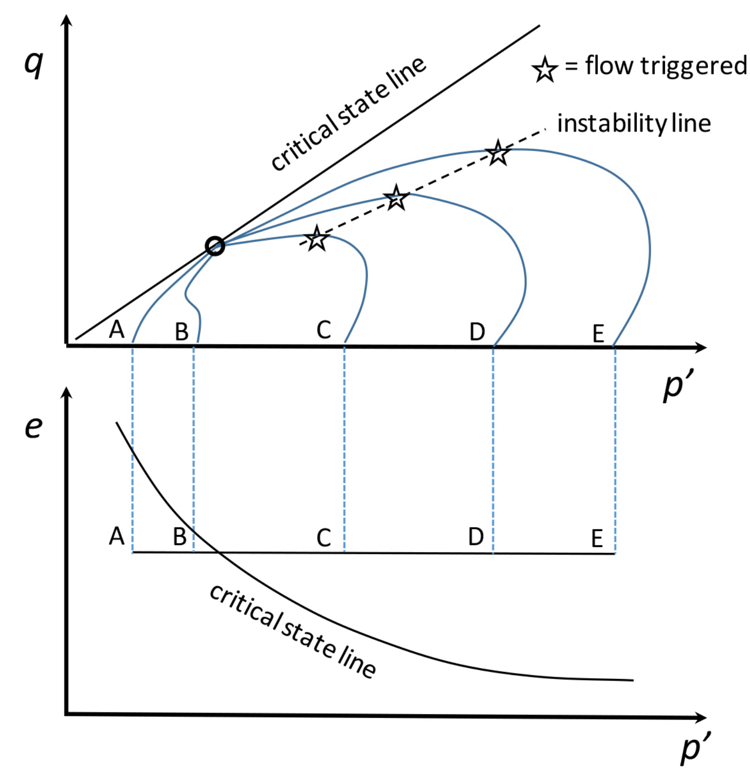

Figure 3. Triggering of flow liquefaction with respect to the critical state line (after Kramer, 1996; Lade, 1999). The top plot shows soil triaxial test results plotted as mean effective stress (p') versus deviatoric stress (q. The bottom plot shows the same results plotted against void ratio (e). All samples achieved steady state "failure" at the critical state line but flow liquefaction occurred along the instability line in contractive soil prior to steady state.

4. Lab and Field Measurements

Two recent studies, supervised by the author, on flow failure and steady state response are described here. The first is a full scale laboratory experiment that captured the residual strength of liquefied soil (Honnett, 2018). In this test a large flexible bucket (1.5 m high by 2.3 m diameter) containing loose saturated Monterey sand was placed on a 10 ton shake table and excited with a harmonic motion at its resonant frequency to induce seismic liquefaction. During liquefaction, in addition to acceleration and pore pressure measurements, a T-bar was pulled through the liquefied soil to measure the steady state shear strength. Prior research (Randolf and Houlsby, 1984; Tokpavi et al., 2008 and 2009) has shown that in a laminar state the flow can be characterized by a closed form solution using a cylinder which the T-bar mimics. Other table top and centrifuge experiments have attempted similar residual strength measurements (de Alba and Ballestero, 2006; Dewoolkar et al., 2016). The shake table results show that for loose ($e>e_{crit}$) uniform sand at a low confining stress of 0.1 atm the steady state residual strength is roughly 1.4 kPa, with a cone penetration resistance of $q_{c1}\approx 0.2$ MPa. Full details on this study are currently under review for publication elsewhere, but the thesis work can be accessed online (Honnette, 2018).

The second study is a field investigation on a seismic induced flow failure from the 2010 M8.8 Chile earthquake (GEER, 2010). Strong ground shaking caused the liquefaction and subsequent flow failure of a tailings dam of mine waste at a defunct gold mine. The 25m high embankment experienced liquefaction at its base resulting in a runout of up to 350 m on shallow slopes. This failure was investigated thoroughly (Moss et al., 2018) and used to develop a detailed case history for future reference (Gebhart, 2017). The failed slope was evaluated against engineering runout distance methods and was back-analyzed to determine an estimate of the steady state residual strength. Here the confining stress conditions were roughly 2 atm and the estimated liquefied residual strength was 8.3 kPa. The soils were measured as contractive ($e<e_{crit}$) based on low cone penetration resistance ($q_{c1}\approx 1.3$ MPa) with respect to Yazdi and Moss (2015) as shown in Figure 4a. Figure 4b shows the results from these investigations plotted against a revised plot of penetration resistance versus liquefied residual strength. The red star is this particular case history with respect to the known database of flow failures (Weber et al., 2015). It should be noted that the analytical "dam break" solution by Hungr (1995) provides an excellent estimate of the observed runout distance of 350 m for this particular failure.

A different study on debris flows was carried out by McKenna et al. (2014). This table top experiment focused on a range of materials that could fail in a debris flow and characterized their properties. The authors used a test mold where the prepared samples could be saturated. The mold is then quickly removed to horizontally load and fail the

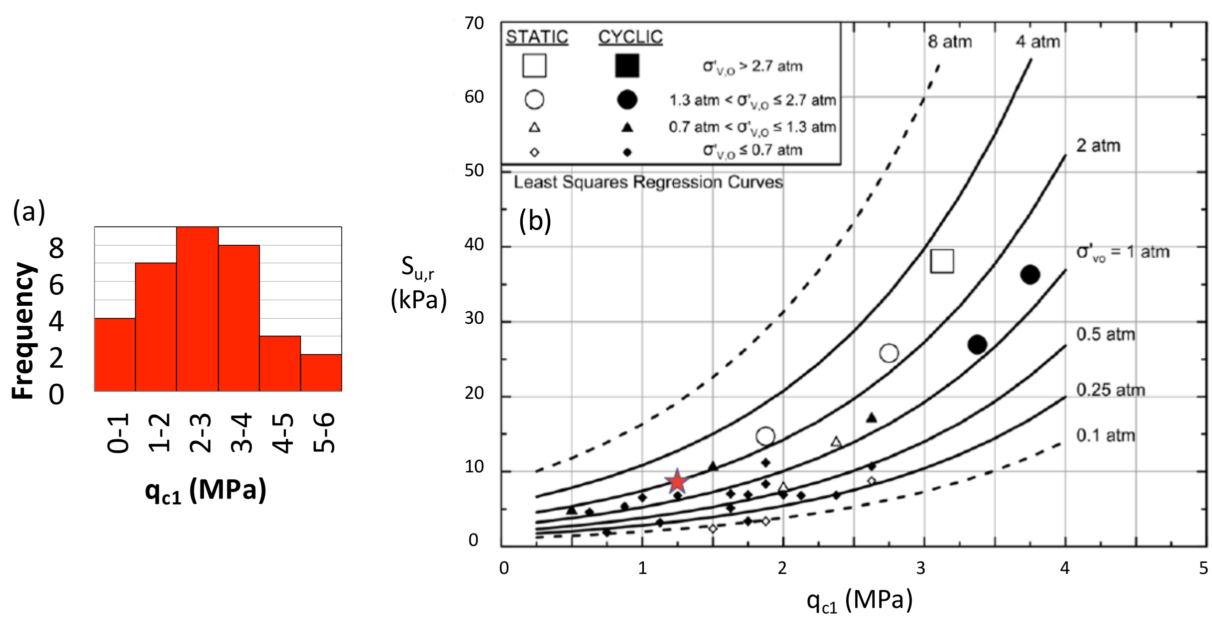

Figure 4. (a) Histogram of cone penetration resistance (q_{c1}) values of flow failure case histories from the Olson & Stark (2002) database (after Yazdi and Moss, 2016). (b) Plot (revised after Weber et al., 2015) correlating penetration resistance to the liquefied residual strength. Red star shows the location of the Las Palmas tailings dam flow failure.

soil in a radial pattern for capturing the failure mode and subsequent deformations. The results generally agreed with large flume experiments (Iverson et al., 2000; Logan and Iverson, 2009). Some of the test results that are pertinent to this discussion are that the density, and hence the void ratio, dictated whether the soil sample would fail as a flow ($e>e_{crit}$) or as a slide ($e<e_{crit}$). [Note: $\rho_d = \rho_s/1+e$ dry density is equal to the density of the solids divided by one plus the void ratio, and $\rho_{sat} = (\rho_s + \rho_w e)/1+e)$ saturated density is equal to the density of solids plus the density of water times the void ratio divided by one plus the void ratio]. Soils that were initially dilatant were capable of dilating past critical state rendering them susceptible to flow during subsequent loading. Failure velocity increased with permeability, and loose soils ($e>e_{crit}$) exhibited higher failure velocities. The analytical "dam break" solution of Hungr (1995) is used here to back-calculate the liquefied residual strength of the samples that were observed to have failed in flow. The equation for "dam break" when rearranged and solved for the liquefied residual strength is:

$$s_{u,r} = 4\left(\frac{\gamma H_o^2 \frac{x_o}{2} x_f - \frac{9}{16}\gamma H_o^2 x_o^2}{x_o^2 x_f - x_f^3}\right) \tag{3}$$

where $s_{u,r}$ is the liquefied residual strength (kPa), γ the unit weight (kN/m^3), H_o the initial height of the "dam" material (m), x_o the initial length of the "dam" material (m), and x_f the runout distance of the flow failure (m). In this simplified solution the initial slope is treated as vertical and the runout shape is treated as a parabola. The liquefied residual strength values from these table top tests at essentially zero confining stress show an average of roughly 6.5 kPa, with a low of 1.7 kPa and a high of 11.9 kPa. The samples are from slope failures sites that covered a range of source materials from gravels to sands (both with fines content) and are representative of the *in situ* field gradations. The liquefied residual strength values from these debris flow materials are in agreement with those observed in tailings flow failure materials and in clean sand liquefaction tests discussed previously.

5. Discussion

In cases of flow failure and debris flows the density or void ratio with respect to the critical density or critical void ratio is a primary controlling variable of flow-like behavior. The *in situ* properties of soil are regularly estimated in engineering situations using cone penetration measurements that are statistically related to engineering properties. Contractive soils exhibit a positive state parameter:

$$\psi = e - e_{crit} \tag{4}$$

For clean sands the state parameter can be estimated using and empirical relationship as found in (Robertson and Cabal, 2014):

$$\psi = 0.56 - 0.33 \log Q_{tn,cs} \tag{5}$$

where $Q_{tn,cs}$ is the stress corrected cone tip resistance of a clean sand, similar to the curves in in Figure 4b but in dimensionless form. So for sandy soils, if they are sufficiently contractive and fully saturated, then flow is the likely failure mechanism which can be forecast using cone penetration measurements.

Fluvially deposited gravels, cobbles, boulders, usually exhibit dilatant behavior due to the nature of the particles and the high energy depositional environment that formed the units. Dilatant material can be pushed into a contractive state by changes in stress as seen in Figure 3 and also to steady state by constant shearing. The propensity for these materials to fail in a debris flow is harder to predict because the flow behavior occurs after large strains and post-peak-strength failure. Here granular kinetics (i.e., granular temperature) is thought to increase the void ratio and the contractive-ness of the material as it tumbles downslope, thereby producing high excess pore pressures and flow condition.

Dry colluvially deposited gravels, cobbles, boulders can exhibit contractive behavior because of the low energy depositional environment that formed these units and therefore can be susceptible to flow type failure when saturated during intense rainfall. Here penetration measurements are not viable because of large particle sized material, but geophysical measurements may be. In soil liquefaction a shear wave velocity of less than roughly 180 m/s (Kayen et al., 2013) is indicative of a contractive soil and subsequent field testing may be useful in refining this value for soils with large particle sizes (e.g., boulders, cobbles, gravels).

As in all these cases the saturation level and contractive behavior are key in determining the likelihood of triggering, post-liquefaction residual strength, and propensity for flow failure.

6. Summary

Presented here are some thoughts on the different phases of flow failures and debris flows, which defines different regions of physics of these failures. Steady state flow with excess pore pressures has been observed to be in common between flow failures and debris flows. The physics of this phase is examined using conceptualized lab results to understand the stress-strain response. Empirical studies of flow failures and debris flows were also examined and the liquefied residual strength were shown to be in rough agreement supporting the argument that this phase is common. Some suggestions were offered as to how best to identify the hazard for different field conditions. The overall goal here is to foster further discussion of their commonalities and to help push hazard mitigation of debris flows and flow failures forward.

Acknowledgements

The author's research on the Chilean flow failure was supported by NRC, SWRI, and CalTrans through the PEER NGL program. The initial investigations of the Chilean flow failure were supported by GEER and NSF. The author's shake table experiments were supported in part by NavFac.

References

Anderson, S. A., and Sitar, N. 1995, Analysis of rainfall-induced debris flows. Journal of Geotechnical Engineering, 121(7), 544-552.

Bryant, S. M., Duncan, J. M., & Seed, H. B. 1983, Application of tailings dam flow analyses to field conditions. Report UCB/GT/83-03, Department of Civil Engineering, University of California, Berkeley, Calif.

de Alba, P., and Ballestero, T. P. 2006, "Residual strength after liquefaction: A rheological approach." Soil Dyn. Earthquake Eng., 26(2–4), 143–151.

Dewoolkar, M., Hargy, J., Anderson, I., de Alba, P., and Olson, S.M. 2016, "Residual and Postliquefaction Strength of a Liquefiable Sand." J. Geotech. Geoenviron. Eng., 142(2): 04015068.

Gebhart, T. 2016, Post-Liquefaction Residual Strength Assessment of the Las Palmas, Chile Tailings Failure. Thesis in partial fulfilment of MS degree. Cal Poly, San Luis Obispo, CA.

GEER. 2010, Geo-Engineering Reconnaissance of the February 27, 2010 Maule, Chile Earthquake. GEER Association Repot No. GEER-022. Berkeley, CA.

Honnette, T. 2018, Measuring Liquefied Residual Strength using Full-Scale Shake Table Cyclic Simple Shear Tests. Thesis in partial fulfilment of MS degree. Cal Poly, San Luis Obispo, CA.

Hungr, O. 1995, "A model for the runout analysis of rapid flow slides, debris flows, and avalanches." Canadian Geotechnical Journal, 32, 610-623.

Iverson, R.M., 1997, The physics of debris flows: Re- views of Geophysics, v. 35, p. 245–296, doi:10.1029 /97RG00426.

Iverson, R.M., 2005, Regulation of landslide motion by dilatancy and pore pressure feedback: Journal of Geophysical Research, v. 110, F02015, doi:10.1029 /2004JF000268.

Iverson, R.M., and Denlinger, R.P., 2001, Flow of variably fluidized granular masses across three-dimensional terrain: 1. Coulomb mixture theory: Journal of Geo- physical Research, v. 106, p. 537–552, doi:10.1029 /2000JB900329.

Iverson, R.M., and LaHusen, R.G., 1989, Dynamic pore- pressure fluctuations in rapidly shearing granular materials: Science, v. 246, p. 796–799, doi:10.1126 /science.246.4931.796.

Iverson, R.M., Reid, M.E., Iverson, N.R., LaHusen, R.G., Logan, M., Mann, J.E., and Brien, D.L., 2000, Acute sensitivity of landslide rates to initial soil porosity: Science, v. 290, p. 513–516, doi:10.1126/science.290 .5491.513.

Jeyapalan, J. K., Duncan, J. M., & Seed, H. B. 1983, Analyses of flow failures of mine tailings dams. Journal of Geotechnical Engineering, 109(2), 150-171.

Jeyapalan, J. K., Duncan, J. M., & Seed, H. B. 1983, Investigation of flow failures of tailings dams. Journal of geotechnical engineering, 109(2), 172-189.

Kayen, R., Moss, R. E. S., Thompson, E. M., Seed, R. B., Cetin, K. O., Kiureghian, A. D., Tanaka, Y., & Tokimatsu, K. 2013, Shear-wave velocity–based probabilistic and deterministic assessment of seismic soil liquefaction potential. Journal of Geotechnical and Geoenvironmental Engineering, 139(3), 407-419.

Kramer, S. L. 1988, Triggering of liquefaction flow slides in coastal soil deposits. Engineering Geology, 26(1), 17-31.

Kramer, M. G. 1996, Geotechnical earthquake engineering. Upper Saddle River, NJ: Prentice Hall.

Lade, P. V. 1999, Instability of granular materials. In Physics and mechanics of soil liquefaction (eds P. V. Lade and J. A. Yamamuro), pp. 3–16. Rotterdam: Balkema.

Logan, M., and Iverson, R.M., 2007, revised 2009. Video documentation of experiments at the USGS debris-flow flume 1992-2006 (amended to include 2007-2009): U.S. Geological Survey Open-File Report 2007-1315, v. 1.1, http://pubs.usgs.gov/of/2007/1315/.

Lucia, P.C., Duncan, J.M., and Seed, H.B. 1981, Summary of research on case histories of flow failures of mine tailings impoundments. Proc. Mine Waste Disposal Technology. Bureau of Mines, Pittsburgh, PA. Informational Circular, 8857. 46-53.

Moss, R.E.S., Gebhart, T.R., Frost, D.J., and Ledezma, C. 2018, Flow Failure Case History of the Las Palmas, Chile, Tailings Dam. PEER Report No. XXXX. Berkeley, CA.

Yazdi, J. S., & Moss, R. E. S. 2016, Nonparametric liquefaction triggering and postliquefaction deformations. Journal of Geotechnical and Geoenvironmental Engineering, 143(3), 04016105.

Randolph, M. G., and Houlsby, G. T. 1984, "The limiting pressure on a circular pile loaded laterally in cohesive soil." Geotechnique, London, England, 34(4), 613-623.

Robertson, P., and Cabal, K. 2014, Guide to Cone Penetration Testing, 6th ed. Gregg Drilling and Testing, Signal Hill, CA.

Schofield, A., & Wroth, P. 1968, Critical state soil mechanics (Vol. 310). London: McGraw-Hill.

Stewart, D.P., and Randolph, M.F. 1994, "T-Bar Penetration Testing in Soft Clay." J. Geotech. Engrg., 120(12): 2230-2235.

Terzaghi, K. (1951). Theoretical soil mechanics. Chapman And Hall, Limited.; London.

Tokpavi, D., L., Magnin, A., and Jay, P. 2008, "Very slow flow of Bingham viscoplastic fluid around a circular cylinder." Journal of Non-Newtonian Fluid Mechanics, 154, 65-76.

Tokpavi, D., L., Jay, P., Magnin, A., and Jossic, L. 2009, "Experimental study of the very slow flow of a yield stress fluid around a circular cylinder." Journal of Non-Newtonian Fluid Mechanics, 164, 35-44.